SPIN-POLARIZED SCANNING PROBE MICROSCOPY

© *R.Laiho, H.Reittu*

Wihuri Physical Laboratory, University of Turku,
20500 Turku, Finland
(Поступила в Редакцию 6 декабря 1995 г.)

Possibility of spin-polarized scanning probe microscopy using a semiconductor tip illuminated with circularly polarized light is theoretically discussed. Both spin-polarized scanning tunneling microscopy and spin-polarized force microscopy are considered. Critical evaluation of working conditions and tip materials suggest that they may provide means to investigate magnetic surface properties of solids with a very high resolution.

Since the invention of scanning probe microscopies (SPMs) including scanning tunneling microscopy (STM) [1] and atomic force microscopy (AFM) [2], imaging of surface structures with single atom resolution has been possible. Along with this development several authors [3–12] have proposed to use the high resolution of STMs for detection of the electron spin contribution to the tunneling current. Accordingly, spin- polarized STMs (SPSTMs) could be constructed for investigations into surface magnetism with ultimate lateral resolution. Recently, feasibility of spin-polarized AFM (SPAFM) has also been considered [13].

A possible way of realizing SPSTMs is to use a ferromagnetic or an antiferromagnetic metallic tip as the source of spin- polarized electrons. This approach is supported by theory [3,14] as well as by experiments [4]. Unfortunately, there are limiting factors like the difficulty in distinquishing the spin-dependent signal from the topographic one and the influence of the stray magnetic field of a ferromagnetic tip to the sample. In an alternative approach to spin-polarized SPM [6,9,13] the tip would be made of a semiconducting material where spin-polarized conduction band electrons can be obtained by pumping with circularly polarized light. According to the calculations performed for a GaAs tip and a ferromagnetic sample a tunneling current or a force sufficient for operation of a spin-polarized STM or AFM, respectively, could be realized. Indeed, recent experimental observations [7,8,10,12] support this approach to SPSTM.

Here we will discuss principles of SPSPM devices with optically pumped semiconductor tips from the viewpoint of Bardeen's [15] tunneling theory. Assuming that the tip is atomically sharp and has a s-type states for creating the tunneling current, the correlation between the SPSTM image and the distribution of the magnetic moments on the surface of the specimen is analyzed.

1. Optically pumped SPM probe

Spin-polarized conduction band (c-band) electrons are created in a semiconducting tip with help of selection rules and intensity ratios of various electronic transitions caused by circularly polarized light (optical pumping) [16]. The degree of the electron spin-polarization (ESP) of a given transition depends entirely on the symmetry of the wave functions involved. For instance, in all III–V zincblende semiconductors direct-gap transitions can be used to produce a photoelectron population in the c-band with equal initial ESP. After photoexcitation the electrons are rapidly thermalized to the band minimum. The majority of the spins of the photocreated electrons are directed parallel or opposite to a unit vector (**n**) along the pumping light beam. The spins are rotated from one direction to the other when the sense of the light polarization is varied between right- and left-hand circular polarization. This feature may be used for separation of the spin-dependent signal component of the tunneling current from that related to topographic properties of the surface. A schematic arrangement of the sample, tip and the pumping laser is shown in Fig. 1.

As an example of III–V semiconductors we consider p-GaAs in which all c-electrons are provided with illumination. The bottom of the c-band and the top of the valence (v) band are located at the centre of the Brillouin zone (Γ-point). The c-band is twofold degenerated with spin. The v-band consists of three twofold degenerated sub-bands, one of which is split off from the others by the spin-orbit splitting Δ. Existence of non-zero Δ is a mandatory condition for achieving finite ESP by optical pumping. However, the remaining degeneracy of the v-band limits the ESP of the photoelectrons to 50%. This restriction can be removed by applying properly oriented stress on the crystal and the value of ESP can be raised near to the theoretical limit of 100%.

The spin-polarization of thermalized photoelectrons is independent of their momentum distribution and may be described with help of a spin-density ma-

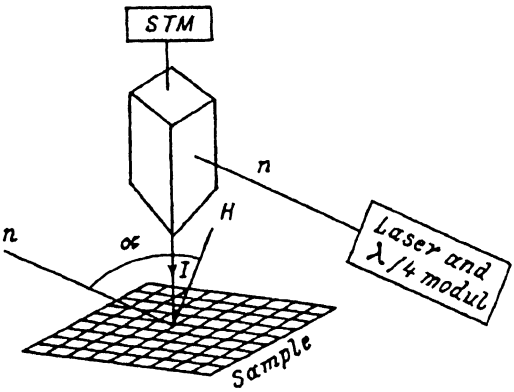

Fig. 1. Schematic arrangement of a semiconducting tip pumped by circularly polarized light.

The vector **n** points along the light beam. The current I consists of photoelectrons with spins polarized alon $\pm n$. The quantization axis of the surface spins is along **H**.

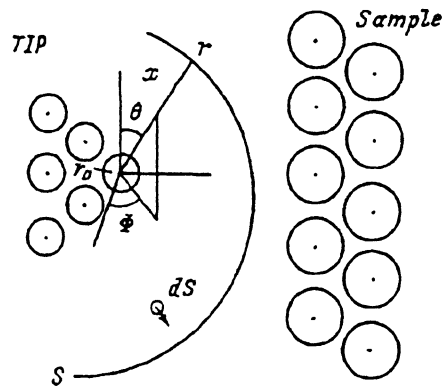

Fig. 2. Schematic representation of the tunneling junction and the separation surface S between the STM tip and the sample.

Exact position and the shape of S are not important. The tip apex atom is at the position r_0, r is a point at S and dS is a surface element on S. The spherical coordinate system (θ, ϕ, x) is also shown.

trix [6,17]

$$\rho = \frac{1}{2}(I + \mathbf{P} \cdot \sigma). \tag{1}$$

Here I is the 2×2 unit matrix and σ is a three component vector with components equal to Pauli matrices. $\mathbf{P}$ is the spin-polarization vector

$$\mathbf{P} = -\mathbf{n} P_0 \sin \xi, \tag{2}$$

where P_0 is a parameter of ESP ($0 \leqslant P_0 \leqslant 1$) and $\sin \xi$ is a factor changing from $+1$ to -1 when the light polarization is switched between right-hand and left-hand helicity. For linearly polarized light $\sin \xi$ is zero.

To achieve a high degree of spin-polarization the photoelectrons should be created near the c-band edge without exciting electrons from the split-off component of the v-band. This means that the photon energy ($\hbar\omega$) must obey the condition $\hbar\omega < E_g + \Delta \approx 1.86$ eV where E_g is the width of the band gap in GaAs. The highest polarization degree is expected when the pumping photon energy is around 1.5 eV [17].

In our previous works [6,9,13] a planar junction was assumed between the tip and the sample. Inside the semiconducting tip the Hamiltonian of the photoelectrons can be written as [6]

$$H_1 = \frac{\mathbf{p}^2}{2m^*} + eU_0, \tag{3}$$

where $\mathbf{p} = -i\hbar\nabla$, m^* is the electron effective mass, and eU_0 is a constant.

The electron wave function can be expressed as

$$\Psi_{E,\alpha}(x) \propto \exp(\pm ikx), \qquad k = \left(\frac{2m^*}{\hbar^2}(E - eU_0)\right)^{1/2}, \tag{4}$$

where α is the spin-index (the wave function has the same form for both spin-projections) and x is the coordinate perpendicular to the junction. We assume that the barrier between the sample and the tip is rectangular [6]. Then the potential changes step-wise from the value eU_0 to eU at the tip surface ($x = 0$) and the Hamiltonian of the electron in the barrier region is

$$H_2 = \frac{\mathbf{p}^2}{2m_e} + eU, \tag{5}$$

where m_e is the free electron mass. When the energy of the electrons is less than the barrier height the wave functions have the form

$$\Psi_{E,\alpha}(x) \propto \exp(\pm \varkappa x), \qquad \varkappa = \left(\frac{2m_e}{\hbar^2}(eU - E)\right)^{1/2}. \tag{6}$$

Inside a ferromagnetic sample we have an effective one-electron Hamiltonian

$$H_3 = \frac{\mathbf{p}^2}{2m'} - \mathbf{H} \cdot \sigma, \tag{7}$$

where m' is the effective mass of the conduction electrons and $\mathbf{H}$ is an exchange field describing their spin-splitting. The corresponding wave functions are

$$\Psi_{E,\alpha}(x) \propto \exp(\pm k_\alpha x), \qquad k_\alpha = \left(\frac{2m'}{\hbar^2}(E \pm H)\right)^{1/2}. \tag{8}$$

This model is supposed to be valid for transition metal ferromagnets [14,18].

In the case of a rectangular potential barrier Eqs. (4), (6) and (8) can be used to find the transmission coefficient of the barrier and the tunneling current in the form

$$I = I_\uparrow + I_\downarrow - (I_\uparrow - I_\downarrow)P_0 \cos\beta \sin\xi, \tag{9}$$

where I_σ is the current component with the spin projection σ and β is the angle between the spins (magnetic moments) of the sample and the light beam $(\mathbf{n})$.

In Ref. [9] a smooth potential barrier with variable form was used to investigate the sensitivity of the spin-asymmetry to the barrier shape. The definitions in Eqs. (3)–(8) are still valid in an asymptotic form inside the tip, as well as inside the sample and the barrier region far away from the interfaces.

Spin-dependence of the tunneling current between an optically pumped tip and a ferromagnetic sample can be analysed using the Bardeen's perturbation approach [15]. Bardeen's tunneling matrix element is expressed by a surface integral

$$M_\sigma = \frac{-i\hbar^2}{2m_e} \int_{\mathbf{S}} (X_\sigma^* \nabla \Psi_\sigma - \Psi_\sigma \nabla X_\sigma^*)\, d\mathbf{S}, \tag{10}$$

where $\mathbf{S}$ is a separation surface located in the middle of the vacuum gap (Fig. 2), $d\mathbf{S}$ is a vector element of $\mathbf{S}$ pointing along the normal of this surface and X_σ and Ψ_σ are the single particle surface wave functions of the tip and the sample, correspondingly.

For a planar junction $\mathbf{S}$ is a plane and the integrand in Eq. (10) is a constant. Then the tunneling matrix element per unit area is [9]

$$M_\sigma = \frac{-i\hbar^2}{2m_e} (X_\sigma^* d\Psi_\sigma/dx - \Psi_\sigma dX_\sigma^*/dx)\Big|_{x=d/2}. \tag{11}$$

where the wave functions are taken in the asymptotic forms that coinside with those in Eq. (6).

The transition probability of an electron from the state X_σ to Ψ_σ per unit time is given by the Fermi's golden rule (see e.g. Refs. [19,20])

$$w_\sigma = \frac{2\pi}{\hbar} |M_\sigma|^2 \delta(E_X - E_\sigma), \tag{12}$$

where E_X and E_y are the energy eigenvalues of the wave functions involved in the transition. The corresponding calculations of the tunneling current [9] show that its spin-asymmetry is highly sensitive to minor changes of the shape of the potential barrier. As will be seen in Chapt. 4 this sensitivity originates from the fact that a SPSTM of this type probes the local spin-density

of the sample surface determined by the spin-components of the surface wave functions. These are very sensitive to the shape of the surface potential.

In Ref. [13] a possible way of realizing an atomic force microscope with spin-resolving properties is analysed. As shown earlier by Chen [21] at the tip-sample separation of 3–6 Å the force acting between a scanning probe and a sample is almost completely caused by the tunneling coupling. This is due to exchange of electrons between the tip and the sample, inducing lowering of the energy levels by an amount equal to the Bardeen's tunneling matrix element $|M|$. This causes an attractive force $-\nabla|M|$ between them. In the case of an optically pumped tip and a ferromagnetic sample the tunneling matrix element is spin-dependent (M_σ in Eq. (11)) and the corresponding force is also spin-sensitive [13]. This force component was estimated to be of the order of 1–0.1 pN which is sufficient for operation of a spin-sensitive atomic force microscope. As far as we know there are until now no experimental results concerning spin-sensitive AFM with an optically pumped semiconductor tip.

2. Spin relaxation

The photoelectrons are accumulated within a surface layer defined by the light absorption depth and the diffusion length of the c-electrons. In p-GaAs both of these lengths are of the order of 1 μm [16]. This means that when the illuminated part of the tip apex has this dimensions roughly homogeneous optical orientation is achieved within its volume.

There exist various relaxation processes diminishing the spin polarization P_I of the conduction electrons acquired at their excitation [17]. Then the polarization can be expressed as $P = (T/\tau)P_I$ with $T^{-1} = \tau^{-1} + \tau_s^{-1}$. To guarantee a significant value of P the semiconductor material should be selected so that the spin relaxation time τ_s is much longer than the carrier life time τ. Another important factor is the diffusion of electrons from the illuminated region to the apex of the tip. The diffusion length of the carriers is $l_e = (D_e\tau_D)^{1/2}$ where D_e is the electron diffusion coefficient and τ_D is their diffusion time. Including this effect the polarization in the tip should be written as $P_{\text{tip}} = (T_t/\tau_D)P_I$ with $T_t^{-1} = \tau_D^{-1} + \tau_s^{-1} + \tau^{-1}$. For efficient operation, the conditions $\tau_D \ll \tau$, τ_S must be fullfilled. To obtain a small value of τ_D the tip should be pumped

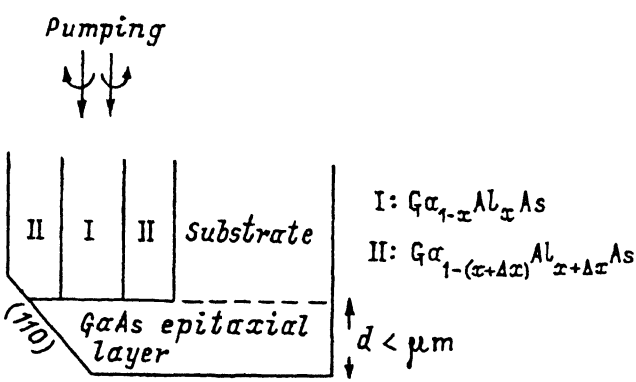

Fig. 3. Proposed construction of a GaAs tip integrated to an end of a $GaAs_{x+\Delta x}As/GaAl_xAs/GaAl_{x+\Delta x}As$ optical waveguide.
The tip apex is formed by a selectively grown GaAs epitaxial layer cleaved at (110) plane.

along its axis, through the sample. This is possible only for semitransparent specimens and limits the direction of the photocreated spins perpendicular to sample surface. To avoid these restrictions the tip can be pumped from aside but then the light beam should be very narrow (less than 1 μm) to limit the distribution of τ_D values.

In Fig. 3 is suggested a tip construction which allows illumination from above. The tip is fabricated by selective epitaxial growth on a GaAs substrate. For optical pumping it is integrated to an end of a $Ga_{1-(x+\Delta x)}Al_{x+\Delta x}As/Ga_{1-x}Al_xAs/Ga_{1-(x+\Delta x)}Al_{x+\Delta x}As$ light guide.

An interesting possibility might be to replace p-GaAs with n-type material. In this case one could utilize instead of carrier diffusion a much faster process, the spin diffusion [17]. Because of the relationship between the diffusion lengths, $l_s \gg l_e$, the problems related to the tip dimensions would be relaxed accordingly. Application of a magnetic field can depolarize or sometimes enhance the spin orientation but the details of this effect depend in a complicated way on the semiconductor material and the geometry of the experiment.

3. Interpretation of an SPSTM image

The one-dimensional treatment of the tunneling current in Chapt. 1 is approximately accurate for a blunt tip having an apex with lateral dimensions much larger than the characteristic length related to the decay constant $\varkappa$ of a surface wave function in vacuum, $\lambda = 2\pi/\varkappa$, which is typically about 6 Å. In the other theoretical works related to SPSTMs [3,14] a similar geometry was used. For achiving a high lateral resolution an atomically sharp tip is required. The corresponding theoretical approach should be three-dimensional including the tip shape. Here we take the first step in this direction by assuming that the tip has a single atom at its apex (Fig. 2).

The spin-dependence of the tunneling current is due to photoelectrons at the edge of the c-band of the tip. That is why we restrict ourselves only to those states when summing over the states of the tip to obtain the tunneling current. The total current is determined by a difference between the current from the filled states of the tip to the empty states of the sample and the current from the filled states of the sample to the empty states of the tip. Below we denote the distribution function of the photoelectrons as $f_0(E)$. The Fermi distribution of the electrons in the sample is defined by the function $f(E) = (1 + \exp(E - E_F)/k_BT)^{-1}$, where T is the temperature, k_B is the Boltzmann constant and E_F is the Fermi energy. The sum over all states of interest can be converted to an energy integral by introducing a density of state factor at the tip, $\rho_T(E)$, and at the sample, $N_\sigma(E)$, respectively.

The part of the tunneling current corresponding to the spin component σ can be expressed as

$$I_\sigma = \frac{2\pi e}{\hbar} \int_0^\infty dE(P_\sigma f_0(E_c+E) - f(E_c-eV+E))\rho_T(E_c+E)N_\sigma(E_c-eV+E)|M_\sigma|^2, \tag{13}$$

where E_c is the energy level of the electrons at the edge of the c-band of the tip, V is the bias voltage, e is the electron charge and $P_\uparrow(P_\downarrow)$ is the probability that the photoelectron spin is parallel to the majority (minority) spin in the sample. For thermalized photoelectrons the expressions of P_σ are given by the

diagonal elements of the spin-density matrix ($P_\sigma = \rho_{\sigma\sigma}$) as (see Eqs. (1), (2))

$$P_\uparrow = \frac{1}{2}(1 - P_0 \cos\beta \sin\xi), \qquad P_\downarrow = \frac{1}{2}(1 + P_0 \cos\beta \sin\xi). \tag{14}$$

The total current of interest, $I = I_\uparrow + I_\downarrow$, is

$$I = I_0 + \int_0^\infty dE \tilde{A}(E) \left(\tilde{\rho}_S - \tilde{m}(\mathbf{r}_0, E) P_0 \cos\beta \sin\xi\right), \tag{15}$$

where I_0 is the part of the current which is independent of the light helicity ($\sin\xi$),

$$\tilde{A}(E) = \frac{\pi e}{\hbar} f_0(E_c) \tag{16a}$$

and

$$\tilde{\rho}(\mathbf{r}_0, E) = N_\uparrow |M_\uparrow|^2 + N_\downarrow |M_\downarrow|^2, \qquad \tilde{m}(\mathbf{r}_0, E) = N_\uparrow |M_\uparrow|^2 - N_\downarrow |M_\downarrow|^2. \tag{16b}$$

Here the coordinates of the center of the tip apex atom, $\mathbf{r}_0$, are simply used as parameters upon which the tunneling matrix elements M_σ depend. In the following we shall show that $\tilde{\rho}$ and $\tilde{m}$ are proportional to the local density of states and the local spin density of the sample at the point $\mathbf{r}_0$ and the energy E.

From Eq. (10) the tunneling matrix elements M_σ are determined through the wave functions of the tip and the sample at the separation surface S. In the Bardeen's method the wave functions at the half-space with interface at S satisfy the Schrцdinger's equation in the vacuum,

$$\left(\nabla^2 - \varkappa^2\right) X_\sigma(r) = 0. \tag{17}$$

A similar equation can be defined for Ψ_σ. Eq. (17) is not valid near the center of the tip apex atom but for calculation of M_σ we need to use only the vacuum tails of the wave functions, which satisfy this equation.

The vacuum tail of the tip wave function can be expanded into spherical-harmonic components $Y_{lm}(\theta, \phi)$, with the nucleus of the apex atom as origin (Fig. 2) i. e. we are looking for the solution of Eq. (17) in the form

$$X_\sigma(r) = \sum_{l,m} C_{lm,\sigma} f_{lm}(\varkappa x) Y_{lm}(\theta, \phi), \tag{18}$$

where C_{lm} are the normalization coefficients and $x = |\mathbf{r} - \mathbf{r}_0|$. The radial functions f_{lm} which decay at large values of $u = \varkappa x$ have the form

$$f_{lm}(u) \propto k_l(u) \equiv (-1)^l \left(\frac{d}{u du}\right)^l \frac{\exp(-u)}{u}. \tag{19}$$

Therefore, a component of the tip wave function with quantum numbers l and m can be written as

$$X_{lm,\sigma}(r) = C_{lm,\sigma} k_l(\varkappa x) Y_{lm}(\theta, \phi). \tag{20}$$

For crystalline surfaces there exist three types of electron wave functions: (*i*) those which correspond to the usual Bloch states inside the solid and decay exponentially in the vacuum side of the interface, (*ii*) surface states and (*iii*) surface resonances. As was shown by Chen [22] the surface states can influence significantly to the imaging mechanism of STM if they are present at the tip.

However, if we assume no surface states or resonances at the tip there remain only the tails of the bulk states that provide the tunneling current. The polarized photoelectrons at the *c*-band edge are responsible of the spin-dependent tunneling. For instance in GaAs this band edge is shaped mostly by the *s* orbitals of Ga-atoms. This is why we take only the spherically symmetric component

$$X_\sigma(\mathbf{r}) = C\exp(-\varkappa x)/(\varkappa x) \tag{21}$$

in the expansion (18). By substituting Eq. (21) into Eq. (10), and taking into account Eq. (18) and the relation

$$\left(\nabla^2 - \varkappa^2\right)\exp(-\varkappa|\mathbf{r}-\mathbf{r}_0|)/(\varkappa|\mathbf{r}-\mathbf{r}_0|) = -\frac{4\pi}{\varkappa}\sigma(\mathbf{r}-\mathbf{r}_0) \tag{22}$$

as well as the Green's theorem transferring the surface integral in Eq. (10) to a volume integral, we can write the Bardeen's tunneling matrix element in the form

$$M_\sigma = \frac{\pi\hbar^2 C}{\varkappa m_e}\Psi_\sigma(\mathbf{r}_0). \tag{23}$$

Here $\Psi_\sigma(\mathbf{r}_0)$ is the sample wave function at the position of the tip apex atom. This is the same result as obtained by Tersoff and Hamann [23] for a spherical tip in the theory of normal STM.

Using Eq. (23) the relations in Eq. (16b) can be written as

$$\tilde{\rho}(\mathbf{r}_0, E) = \tilde{C}^2\left(N_\uparrow|\Psi_\uparrow(\mathbf{r}_0)|^2 + N_\downarrow|\Psi_\downarrow(\mathbf{r}_0)|^2\right), \tag{24a}$$

and

$$\tilde{m}(\mathbf{r}_0, E) = \tilde{C}^2\left(N_\uparrow|\Psi_\uparrow(\mathbf{r}_0)|^2 - N_\downarrow|\Psi_\downarrow(\mathbf{r}_0)|^2\right) \tag{24b}$$

with the coefficient

$$\tilde{C} = \frac{\pi\hbar^2 C}{\varkappa m_e}. \tag{24c}$$

Eq. (24b) has an obvious physical meaning. Namely, if E_n is the energy eigenvalue of an electron in the sample, the local spin density at the point $\mathbf{r}$ and the energy E is

$$m(\mathbf{r}, E) = \frac{1}{2\Delta E}\sum\left(|\Psi_{n\uparrow}(\mathbf{r})|^2 - |\Psi_{n\downarrow}(\mathbf{r})|^2\right)$$

$$E - \Delta E \leqslant E_n \leqslant E + \Delta E \tag{25}$$

when $\Delta E \to 0$. This can be written as

$$m(\mathbf{r}, E) = \frac{1}{2\Delta E}\int_{E-\Delta E}^{E+\Delta E} dE\left(N_\uparrow(E)|\Psi_\uparrow(\mathbf{r})|^2 - N_\downarrow(E)|\Psi_\downarrow(\mathbf{r})|^2\right). \tag{26}$$

At the limit $\Delta E \to 0$ we have from Eq. (26)

$$m(\mathbf{r}, E) = N_\uparrow(E)|\Psi_\uparrow(\mathbf{r})|^2 - N_\downarrow(E)|\Psi_\downarrow(\mathbf{r})|^2. \tag{27}$$

Analogously $\tilde{\rho}_S$ in Eq. (16b) is proportional to the local density of the sample states $\rho_S(\mathbf{r}_0, E)$. Usually the photoelectron energies are restricted to about 10^{-2} eV above the c-band edge. Within this range $m(\mathbf{r}_0, E)$ and $\rho(\mathbf{r}_0, E)$ can be considered as constants. Thus it is possible to write with help of Eqs. (16a), (16b) and (27)

$$I = I_0 = A[\rho(\mathbf{r}_0, E) - \mathbf{P} \cdot \mathbf{m}(\mathbf{r}_0, E) - \mathbf{P} \cdot \mathbf{m}(\mathbf{r}_0, E_c - eV) \sin \xi], \tag{28}$$

where $A = \tilde{C}^2 \tilde{A}$ and $\mathbf{m}(\mathbf{r}_0, E)$ is a vector pointing along the majority spin direction on the sample surface and having the modulus equal to $m(\mathbf{r}_0, E)$.

In Eq. (28) I_0 is independent of the sense of light polarization. However, it can be affected by the pumping light that causes charge accumulation at the semiconductor tip giving rise to the surface photovoltage effect [24] (SPV). One clear manifestation of SPV is that a STM with a proper semiconductor tip can be operated under illumination without an applied bias voltage between the tip and a sample [11]. At small light intensities SPV grows rapidly with pumping power but at higher excitation levels, that are available in STM configurations, it saturates and we can consider I_0 as a constant with respect to the light excitation. This makes it possible to measure the magnitude of $\mathbf{m}(\mathbf{r}_0, E)/\rho_S(\mathbf{r}_0, E) \equiv \mathbf{P}_S(\mathbf{r}_0, E)$ which is the degree of the spin-polarization of the sample surface. It is enough to use two excitation intensities (1) and (2) within the range of saturation of SPV. Switching of the light intensity causes changes in the tunneling current I in Eq. (28). Firstly by using linearly polarized light ($\sin x = 0$) the change of I is

$$\delta I_0 = (A_1 - A_2)\rho_S(\mathbf{r}_0, E), \tag{29}$$

where the subscript of A refers to the excitation level. For circularly polarized light the change of the tunneling current oscillations caused by the modulation of $\sin \xi$ between $+1$ and -1 is

$$\delta I_{pm} = -2(A_1 - A_2)\mathbf{P} \cdot \mathbf{m}(\mathbf{r}_0, E). \tag{30}$$

Thus we find

$$\mathbf{P} \cdot \mathbf{P}_S(\mathbf{r}_0, E) = -\frac{1}{2}\frac{\delta I_{pm}}{\delta I_0}, \qquad \mathbf{P}_S(\mathbf{r}_0, E) = \frac{\mathbf{m}(\mathbf{r}_0, E)}{\rho_S(\mathbf{r}_0, E)}. \tag{31}$$

If the value of the local density of state factor $\rho_S(\mathbf{r}_0, E)$ is available from an independent measurement that of $\mathbf{m}(\mathbf{r}_0, E)$ can be determined.

In such experiment SPV can be measured independently [10] and its effect on the energy of the tunneling electrons can be taken into account. However, the SPV is accompanied with the band bending near the tip surface. This is not desirable since it leads to photoelectron accumulation on the tip surface where their ESP is lowered by long life time. The result of Ref. [10] indicate that the band bending can be reduced by using a high doping level in the tip.

For instance in p-GaAs doped with $1.3 \cdot 10^{19}\,\mathrm{cm}^{-3}$ Zn impurities this effect was not noticeable and the influence of SPV should be negligible.

We can see from Eq. (28) that in the simplest case of the s-type tip state the corrugation of an SPSTM image is due to changes of the local spin density at the position of the tip apex atom and at the energy of the tunneling electron. Such corrugations of the local spin densities have been calculated numerically for several magnetic surfaces and overlayers [25] by using the full potential linearized augmented plane wave (FLAPW) method. It should be noted that the corrugation of $m(\mathbf{r}, E_\mathrm{F})$ differes from that of the local spin-density (or magnetization) $m(\mathbf{r})$, which is normally used in literature to represent results of numerical calculations on magnetic surfaces. For instance, at clean bcc Fe(110) surface a large positive (parallel to the majority spin) spin-polarization is found around the atomic sites [25]. Their polarization is notably enhanced toward the vacuum side, which is typical of magnetism with weakened interatomic interactions (e.g. at interface with vacuum). On the other hand, the calculated $m(\mathbf{r}, E)$ is negative at the surface and despite of the enhancement of the surface magnetic moment over the bulk value, SPSTM is expected to see a negative spin-polarization on this surface [25]. Actually the same conclution can be made for all surfaces of the 3d ferromagnets (Fe, Co and Ni).

One suprising result is that oxygen absorbates on Fe(110) surface are cabable to change the sign of $m(\mathbf{r}, E_\mathrm{F})$ from negative to positive in the vacuum region [25]. Another point is that on some surfaces and overlayers (e.g. Fe/Ni(111) and Ru/Ag(001)) $m(\mathbf{r})$ is highly corrugated in atomic scale while $m(\mathbf{r}, E_\mathrm{F})$ remains nearly constant [25]. Obviously such magnetic structures show no atomic features when investigated with SPSTM. When selecting a sample surface or an overlayer for a SPSTM study we cannot use the calculated local magnetization ($m(\mathbf{r})$) as a guide since this is not the magnitude that SPSTM probes. Instead, the surface should have highly varying local spin-density at a given energy available in the tunneling experiment. UHV conditions are desirable since $m(\mathbf{r}, E)$ of a clean surface could be masked by absorbants.

A method similar to scanning tunneling spectroscopy of electronic states might be used to investigate surface magnetization $\mathbf{m}(\mathbf{r}_0)$ or the distribution of its spin-polarization $\mathbf{P}_S(\mathbf{r}_0)$. It may be called «spin-polarized scanning tunneling spectroscopy» and it should involve measurement with different values of the bias voltage at each position of the tip. Then the magnetic information can be obtained as described in Eqs. (29 - 31). An integrated picture would present a map of $\mathbf{m}(\mathbf{r}_0)$ or $\mathbf{P}_S(\mathbf{r}_0)$.

4. Experimental progress towards SPSPM using semiconducting tips

Eq. (9) predicts that at pumping power 5 mW on a 10 μm wide spot the photoinduced tunneling current density would be of the order of 0.1 $\mathrm{nA/nm}^2$ [6]. Also the spin-asymmetry of the tunneling current should be detectable with present STM techniques.

According to recent experiments it is quite possible to achive atomic resolution with STMs using p-GaAs tips of $10^{17} - 10^{18}\,\mathrm{cm}^{-3}$ doping density. The authors of Ref. [8] report about preparation of a p-GaAs tip (Zn-doped, $1.2 \cdot 10^{19}\,\mathrm{cm}^{-3}$ material) simply by cleaving a single crystal wafer along the

(110 and (1$\bar{1}$0) directions which are at right angles to each other and to (100) plane. The tip formed by a corner of these facets was sharp enough to image the Si(111)–7 × 7 surface reconstruction in UHV. Similarly, photoinduced tunneling current of the order of several hundred pA was obtained from a *p*-GaAs tip upon HeNe (638.8 nm) excitation [10]. In this experiment atomic resolution of highly oriented pyrolytic graphite surface was observed under optical excitation. In Ref. [12] preparation of a GaAs microtip by epitaxial growth on properly selected substrate is described. This method is interesting [6] since it provides a way to prepare tips which are strained by the lattice mismatch between the epitaxial layer and the substrate. In a strained GaAs (001) layer grown by the MOCVD method on GaP_xAs_{1-x} ESP of photoelectrons as high as 86% has been achived by optical pumping [26].

It has also been demonstrated that spin-polarized tunneling current can flow between a ferromagnetic (Ni) STM tip and a GaAs sample pumped by circularly polarized light. This was done by modulating the sense of the light polarization and observing corresponding oscillations of the tunneling current. An advantage of using a semiconducting tip in spin-polarized STM experiments is the substantial increase of the sensitivity by use of the modulation technique combined with phase sensitive detection.

The surface photovoltaic effect of a photosensitive GaAs probe has been used for near-field magneto-optical imaging [27]. In this experiment alternation of the optical transmission of a thin magnetic layer was observed when modulating the light helicity between right- and left-hand circular polarization (magnetic circular dichroism). It was possible to image magnetic bits, written in a Pt/Co multilayer, with 250 nm lateral resolution. Magneto-optical effects depend on bulk magnetization whereas the spin-polarized tunneling is sensitive to spin-density of the electronic states at the sample surface. These two contributions can be distinquished by analyzing their dependence on the excitation wavelength, surface preparation, and the bias voltage. The authors of Ref. [27] conclude that by using semiconducting (e.g. *p*-GaAs) tips, it would be possible to construct a versatile SPM that is capable to measure simultaneously sample topography, bulk magnetization and surface spin-density with subnanometer resolution.

Principles of spin-polarized scanning tunneling microscopy and spin-polarized force microscopy employing optically pumped semiconductor tips are theoretically analysed. The values of the spin-dependent tunnel current and that of the spin-dependent force calculated for a GaAs tip and a ferromagnetic sample are within the detection limits reported for presently existing conventional scanning probe microscopes. The predicted tunnel current agree also reasonably with the first experimental results for photoamperic probes.

A method for determining the local distribution of surface magnetic properties is suggested including spin-polarized scanning tunneling spectroscopy. This involves proper consideration of the pumping light polarization, physical meaning of the tunneling matrix element as well as the possible surface photovoltage due to charge accumulation in the illuminated semiconductor tip.

Several recent experiments show that single atom resolution can be obtained with a scanning tunneling microscope using a semiconductor tip. This suggests that construction of spin-polarized scanning probe microscopes with subnanometer resolution is quite feasible. Another interesting possibility is to use an illuminated semiconductor tip for near-field magneto-optical imaging of magnetic films, superconductor films etc.

The authors are grateful to Prof. Vladimir Fleisher for illuminating discussions. This work is supported by Prof. Väinö Hovi Foundation and Ella och Georg Ehrnrooths Stiftelse.

References

[1] Binnig G., Rohrer H., Gerber Ch., Weibel E. Phys. Rev. Lett. **49**, 57 (1982).
[2] Binnig G., Quate C.F., Gerber Ch. Phys. Rev. Lett. **56**, 930 (1986).
[3] Minakov A.A., Shvets I.V. Surf. Sci. **236**, 377 (1990).
[4] Wiesendanger R., Güntherodt H.-J., Güntherodt G., Gambino R.J., Ruf R. Phys. Rev. Lett. **65**, 247 (1990).
[5] Molotkov S.N., Pis'ma Zh. Eksp. Teor. Fiz. **55**, 180 (1992).
[6] Laiho R., Reittu H.J. Surf. Sci. **289**, 363 (1993).
[7] Sueoka K., Mukasa K., Hayakawa K., Jpn. J. Appl. Phys. **32**, 2989 (1993).
[8] Nunes G., Jr. Amer N.M. Appl. Phys. Lett. **63**, 1851 (1993).
[9] Reittu H.J. J. Phys. Condens. Matter **6**, 1847 (1994).
[10] Jansen R., van der Wielen M.C.M.M., Prins M.W.J., Abraham D.L., van Kempen H. J. Vac. Sci. Technol. **B12**, 2133 (1994).
[11] Manassen Y. Adv. Mater. **6**, 401 (1994).
[12] Yamaguchi K., Okamoto K., Yugo S., J. Appl. Phys. **77**, 6061 (1995).
[13] Reittu H.J. Surf. Sci. **334**, 257 (1995).
[14] Slonczewski J.C. Phys. Rev. **B39**, 6995 (1989).
[15] Bardeen J. Phys. Rev. Lett. **6**, 57 (1961).
[16] Pierce D.T., Celotta R.J. Optical Orientation / Ed. F. Meier, B.P. Zakharchenya. North–Holland. Amsterdam (1984). P. 259.
[17] Dyakonov M.I., Perel V.I. Ibid. P. 11; G.E. Pikus, A.N. Titkov. Ibid. P. 73; V.G. Fleisher, I.A. Merkulov. Ibid. P. 173.
[18] Stearns M.B. J. Magn. Magn. Mater. **5**, 167 (1977).
[19] Feuchtwang T.E., Cutler P.H. Physica Scripta **35**, 132 (1987).
[20] Reittu H.J., Am. J. Phys. **63**, 940 (1995).
[21] Chen C.J. J. Phys. Condens. Matter **5**, 1227 (1991).
[22] Chen C.J., Introduction to Scanning Tunneling Microscopy Oxford University Press. N.Y. (1993). P. 75.
[23] Tersoff J., Hamann D.R. Phys. Rev. **B31**, 805 (1985).
[24] Hecht M.H. Phys. Rev. **B41**, 7918 (1990).
[25] Wu R., Freeman A.J. Phys. Rev. Lett. **69**, 2867 (1992).
[26] Nakanishi T., Aoyagi H., Horinaka H., Kamiya Y., Kato T., Nakamura S., Saka T., Tsubata M. Phys. Lett. **A158**, 345 (1991).
[27] Prins M.W.J., Groeneveld R.H.M., Abraham D.L., van Kempen H., van Kesteren H.W. Appl. Phys. Lett. **66**, 1141 (1995).